HYDROTHERMAL WAVES IN DROPLET EVAPORATION

Zhong, X, Ho A. and Duan F.*
*Author for correspondence
School of Mechanical and Aerospace Engineering,
Nanyang Technological University,
Singapore, 639798
E-mail: feiduan@ntu.edu.sg

ABSTRACT

The hydrothermal waves (HTWs) have been investigated on the evaporation of ethanol, novec-7100 and pure water sessile droplets forming at the top of a cone-shaped container under the steady state. For ethanol and novec-7100, the temperature along the droplet diameter is higher near the triple line than in the middle section, within which the temperature shows slight oscillations representing instability of the thermal motion. Behaving inversely, the temperature of the water droplet is higher in the middle section than at the periphery, and no evident oscillation is observed. The results show that with the increase of the imposed voltage, the thermal motion is more rapid and the number of HTWs is increased in ethanol and novec-7100. The relation between the number of HTWs and the imposed voltage is fitted by an empirical equation for novec-7100. With analysis of the origin of HTWs, the droplets evaporation belongs to the category of HTWs type 1 with gravity prevails over the surface tension.

NOMENCLATURE

g	[m/s^2]	Gravitational acceleration
h	[m]	Droplet height
N_W	[-]	Number of HTWs
R	[m]	Droplet contact line diameter
T	[°C]	Temperature
V_e	[V]	Voltage
α	[m^2/s]	Thermal diffusivity
β	[1/K]	Thermal expansion coefficient
γ	[mN/mK]	Surface tension coefficient
ΔT	[°C]	Temperature difference
μ	[ms/m^2]	Kinematic viscosity
σ	[mN/m]	Surface tension

INTRODUCTION

Droplet evaporation is a ubiquitous phenomenon in nature, biology and industry. It is a process combining heat transfer and phase-change that can be frequently seen in the cycle of water in nature, combustion, printing, coating, spray cooling, to cite just a few cases [1,2] So far countless investigations have been contributed to the evaporation of sessile droplets with combination of the evaporation and dynamics of the three-phase line. A pinning contact line, for instance, leads to a more rapid evaporation rate as compared to a depinning one for the droplet with the same initial wetting area. [3] When a droplet keeps pinning on a substrate, the evaporation flux is non-uniform and diverges near the droplet edge, resulting in a surface gradient and a consequent Marangoni flow which could be the origin of the hydrothermal waves (HTWs).

HTWs are thermally induced traveling waves in the liquid. Smith and Davis firstly predicted the type of thermocapillary instability as they studied the stability of a thin fluid layer which owns a free surface with an interfacial temperature gradient [4]. They demonstrated that unstable fluid layers, subjected to sufficiently large horizontal temperature gradients, generated steady longitudinal rolls and unsteady HTWs. Riley and Neitzel managed to demonstrate the existence of HTWs in a layer of silicone oil experimentally [5]. Recently, HTWs have attracted growing attentions and they have been frequently observed in volatile liquids, such as ethanol, methanol, FC-72, etc. Initially, HTWs were discovered in shallow containers with cylindrical or rectangular shape with the imposed temperature gradient [6,7]. They were found to propagate from one side to another. Afterward, HTWs in sessile droplets associated with the thermal patterns have been studied under both normal and micro-gravity conditions [1,2,8,9]. The thermocapillary instabilities have been probed by using an infrared technique in evaporating droplets with simultaneous recording of the heat and mass transfer, shape evolution, thermal patterns, and liquid-solid temperature field. It has been found that the number of waves reduced nonlinearly with time for collapsing droplets, and that increasing the temperature gradient led to more HTWs However, the previous study of HTWs focused on the shrinking sessile droplets, the interface change could be affect HTWs. The steady-state droplet evaporation experiments also showed a strong temperature variation from the centerline to the edge [10,11]. Thus, our present work is to investigate the HTWs in stable sessile droplets of water when the syringe pump can cautiously supply the working fluids (ethanol, novec-7100, and water) to maintain the liquid interface above a funnel with the circular-shaped mouth. The temperature distribution is recorded for HTW analysis for the evaporating droplet as the funnel wall is heated.

EXPERIMENTAL METHODS

The evaporation of a sessile droplet sitting on the funnel mouth is recorded by an infrared thermographic camera amounting on the top of the droplet. Figure 1 shows the schematic of the experimental configuration. The working fluids were pumped into the funnel by the syringe pump until a droplet can be formed on the cone-shaped funnel. The wall of the funnel was heated by a heat tape and voltage can be

controlled by a DC power supplier. At the certain heating power input, the syringe pump was adjusted to keep the constant maximum droplet height observed at the side-view. It took roughly 20 minutes for the droplet to reach a steady state of evaporation. Then the pumping rate was a fixed with a constant droplet height. The working fluid evaporation rate would equal the supplied rate from the syringe pump. The temperature distribution at droplet surface was recorded from top view by the IR camera. The obtained repeating thermal patterns in respect with time were processed by executing the IRBIS 3 plus programming.

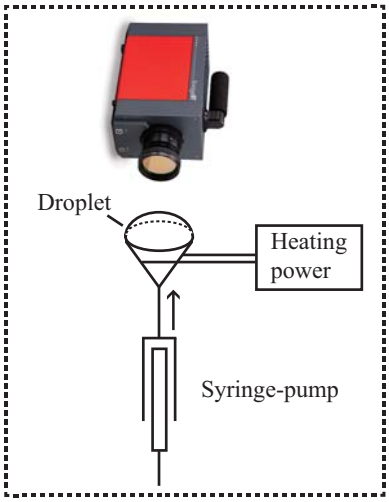

Figure 1: The schematic of the experimental setup.

Two volatile liquids, pure ethanol (99.9 %) and novec-7100 from Sigma Inc. were selected to investigate the HTWs while pure deionized water is employed as a reference. These three kinds of liquids with different properties of volatility, surface tension, viscosity and latent heat were expected to show distinctly different thermal motions during the quasi-steady evaporation. The transparency of pure water and semi-transparency of ethanol and novec-7100 in terms of the wavelength range of the IR camera permit the visualization of thermal patterns at the liquid-vapor interface. The funnel was made of stainless steel with diameter ($2R$) at 24 mm at mouth. The edge of the cone container was heated by an electric resistance belt and regulated with the voltage and current by the electric power source. The IR camera (InfraTec 8300, 640×512 pixels) fitted with a standard lens with visualization of a field of view of 21.7×17.5 mm^2 is set to record the droplet with a frequency of 1 frame every 10 ms.

The experiments were conducted under the open conditions with the atmospheric pressure at 1 atm, the temperature at 22±1°C, and the humidity of 40±5%. The liquid in the funnel was heated with a voltage from 0 V to 12 V for novec-7100, 0 V to 14 V for ethanol, and 0 V to 16 V for pure water. The upper limit of the voltage is constrained by the boiling point of each liquid. Calibration of IR camera is conducted before the experiments by measuring the inner wall temperature with adjustment of the supplied voltage.

RESULTS AND DISCUSSION

Temperature Distribution in the Droplet Evaporation

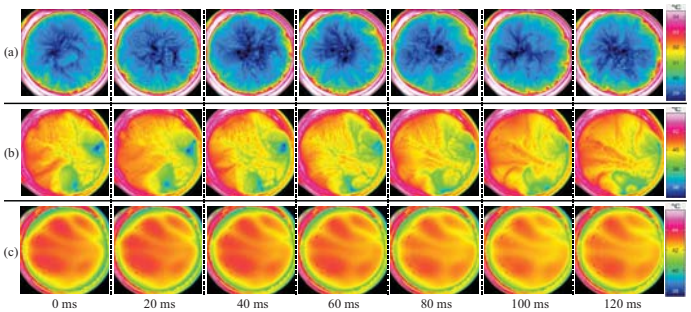

Figure 2: Thermal patterns of (a) novec-7100 (b) ethanol, and (c) water droplets during evaporation for a period of 120 ms with a supplied voltage at 12 V.

The temperature was measured with the IR camera in each of experiments. Intense thermal motions in term of temperature distribution have been observed in ethanol and novec-7100 droplets but the pure water one. As presented by Figures 2 (a and b), rapid thermal convection evolves periodically with space and time even though the side view of droplet profiles were stable under steady state. The cold liquid tends to be driven to the center at the liquid-vapor interface, and then sinks; as replenishment, the liquid near the three-phase line ascends to fulfil the convective circulation. As soon as the quasi-steady state of evaporation is reached, the temperature near the triple line is higher than the one in the center, based on the visualization of the IR camera. The thermal pattern was not very symmetric due to the imperfectly uniform heating of the funnel edge. In spite of that, it is visualized through the IR camera that the temperature in the central region remains lower than that in the vicinity of the edge. As the central region is far from the heated area and has a greater thickness leading to a larger thermal resistance, it should be the coldest point of the droplets for ethanol and novec-7100. The local evaporation also maintained the interfacial temperature variation under steady state. As a result, the large-scale induced convection flow is induced by the temperature field.

The water droplet, however, displays a distinctly different thermal pattern that no obvious convective flow has been observed in the open condition due to higher latent heat (see Figure 2 (c). Despite that the three-phase line is heated, the region near it has a lower temperature as compared to the central area, which may due to the evaporation-induced cooling or small-scale convection near the triple line. Besides, according to Hu and Larson [13] even few contaminants at the free surface enable the almost entire suppression of Marangoni flow in an evaporating water droplet, which as well could be the reason for the absence of convective flow observed in our experiments conducted in the open conditions.

The repeatable temperature distribution as a function of normalized radius can be seen in Figure 3. The overall temperature increases with the imposed voltage. As the voltage is 0 V, the temperature roughly constant. A slight temperature increase was found in the experiment with 6 V. At the voltages of 8 V or above, the temperature close to periphery is higher

than that at centerline. With an increase of power input, the difference has a trend to increase. Above 18 V, the boiling was observed in the experiments. The data are not included.

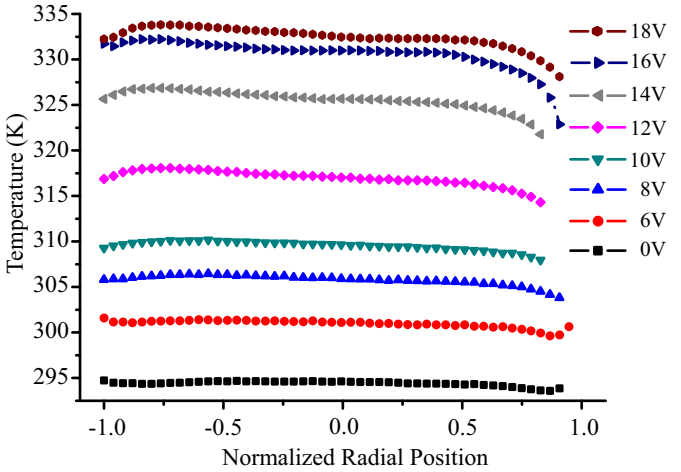

Figure 3: Temperature fields along the diameter of the water droplets under the supplied voltage ranging from 0V to18V.

However, the temperature distribution in Figure 4 for ethanol and Figure 5 for novec-7100 illustrates the difference tendency in comparison with water. The temperature field is plotted along the diameter of the droplet for ethanol and novec-7100. Although the overall temperature increases with the imposed voltage, the temperature near the triple line is obviously higher than the one away from the periphery for each of voltage input. Under the same voltage, the temperature profile is more parabolic in the droplets of novec-7100. In addition, the temperature shows slight oscillations from roughly -0.8*R* to 0.8*R* for both ethanol and novec-7100, revealing the non-uniformity of the thermal pattern led by existence of HTWs. The temperature line does not display obvious oscillations in the water droplets.

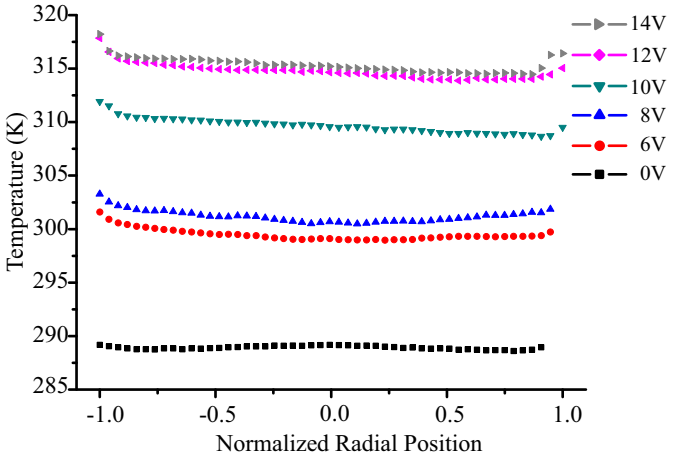

Figure 4: Temperature fields along the diameter of the ethanol droplets under the supplied voltage ranging from 0V to 14V.

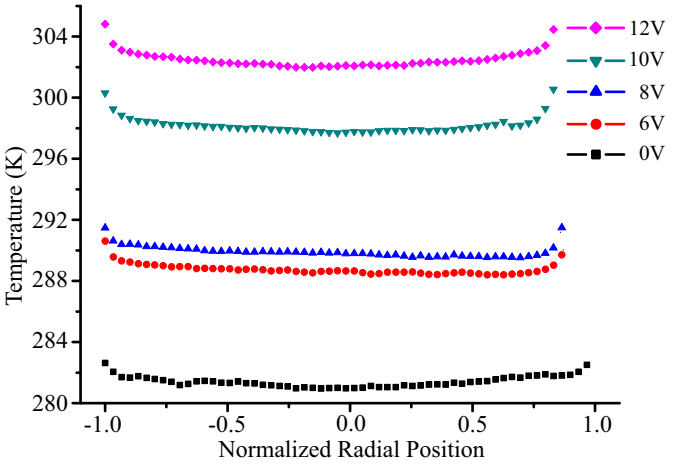

Figure 5: Temperature fields along the diameter of the novec-7100 under the supplied voltage ranging from 0V to 12V.

One concern in terms of the ethanol and novec-7100 droplets evaporation is the adsorption of water vapor from humid air crossing the free surface into the liquid phase. Since the experiments were conducted under a temperature T=22±1°C and a humidity of 40±5%, the dew point corresponding to a wet-bulb temperature is about 7.8°C, which is higher than the minimum apex temperature at about 13°C for ethanol and 9°C for novec-7100. Therefore, adsorption of water vapor into droplets can be excluded from the interpretation.

Hydrothermal Wave in the Droplet Evaporation

Figure 2 shows a strong wave is form in ethanol and novec-7100, but not in the water. The analysis of hydrothermal wave is conducted only for ethanol and novec-7100. The characteristic length is determined based on the geometry of the circular funnel. Since the distance between the interface and funnel inlet at bottom of the funnel is relatively long for the slow evaporation rate in the open conditions, the disturbance caused by the inlet velocity is assumed to be eliminated due to the liquid in the container working like a buffer and helping stabilize the system. We only focus on the droplet sitting above the funnel mouth, and ignore the influence of the cone-shaped liquid below the droplet cap on the funnel mouth. Therefore, the maximum thickness, *h*, in the centerline of the droplets and the radius the circular funnel mouth, *R*, are selected in the calculation.

Different regimes for thermocapillary and thermogravity flow depending on the fluid depth, h, was categorized in Refs [2, 14] and listed in Table 1. According to the dynamic bound number, B_d , representing the ratio of Rayleigh number ($Ra = \frac{\beta g \Delta T h^4}{\gamma \alpha R}$) and Marangoni number ($Ma = \frac{\gamma \Delta T h^2}{\mu \alpha R}$) and the static bound number, $Bo = \frac{\rho g h^2}{\sigma}$, the nature of the thermal motion can be determined. Therefore, relevant dimensionless numbers are calculated to define the thermal flow. Table 1 lists

the values of *Bo*, *Ra*, *Ma*, and B_d for ethanol and novec-7100 droplets, where the coefficient of surface tension is $\gamma = \frac{d\sigma}{dT}$.

Table 1 Categorization of the thermal regimes depending on B_d and *Bo* [2,14].

$B_d > 1$	Stationary Rolls – Thermogravity flow		
$B_d < 1$	Hydrothermal Waves Thermocapillary flow	*Bo*<1	HTWs 2 Capillary flow
		Bo>1	HTWs 2 Gravity flow

Table 2 The values of dimensionless numbers for ethanol and novec-7100 from average temperature difference.

Number	*Bo*	*Ra*	*Ma*	B_d
ethanol	1.34	334	1164	0.29
novec-7100	1.09	565	1536	0.37

From the values of B_d and *Bo* for ethanol and novec-7100 from Table 2, the corresponding cases fall at the category of HTWs type 1 dominated by thermocapillary flow. The B_d values defined as the ratio of *Ra* to *Ma* reveals the ratio of thermogravity and thermocapillary. B_d is smaller than 1 for ethanol and novec-7100 in the present experiments, suggesting that the thermal patterns are mainly driven by thermocapillary flow. As *Bo* is slightly over 1 for both the liquids, the gravity force plays competitive roles as compared to that of the surface tension force.

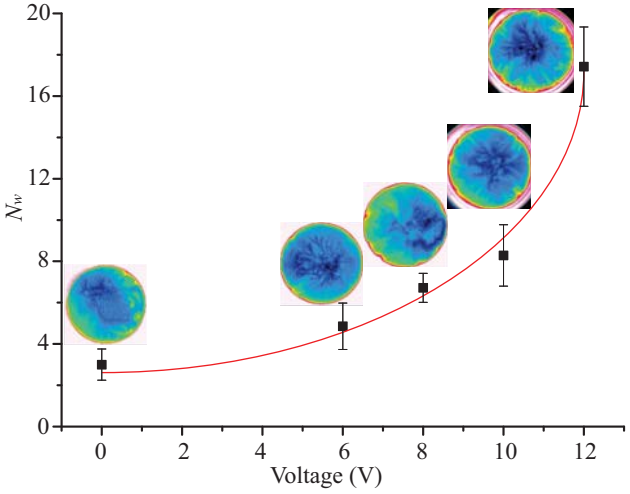

Figure 7: The change of the number of HTWs with the supplied voltage. The insets are the corresponding thermal patterns at different voltage values.

The spontaneous development of HTWs takes place in the quasi-steady state of evaporation. The petal-like patterns are organized asymmetrically due to the imperfect heating conditions. The number of HTWs, N_W, is calculated for novec-7100 by employing the method proposed by Sobac and Brutin [2] and the relation with the imposed voltage is drawn in Figure 7. The petal-like pattern in the vicinity of the three-phase line increasing with an increase of the voltage is consistent with the driving mechanism of HTWs that a larger temperature gradient would intensify the driving force and thereby increase the HTWs. The trend of NW with the imposed voltage is fitted and expressed as,

$$N_w = 2.94 + 0.22e^{0.35V_e} \quad (1)$$

where V_e is the voltage value.

CONCLUSION

We experimentally studied the thermal motion in evaporating ethanol, novec-7100 and water droplets forming on the top of a funnel with the circular mouth. By employing an IR camera to visualize the thermal field and a heating power to heat the droplet edge, the evaporation process was recorded and analyzed by evaluation of the dimensionless numbers. The number of HTWs was increased by enlarging the supplied voltage, and the relation between them was fitted by an empirical equation. The problem in our study stays in the category of HTWs type 1. The temperature gradient at the liquid-vapor interface induced a surface tension gradient which drove the hot liquid to the colder region, leading to thermal-convective-flow. The temperature along the droplet diameter was higher near the triple line for ethanol and novec-7100, and it exhibits the oscillations in the middle section of the droplet. While for the pure water, the temperature was higher in the middle section despite that the droplet was heated at the periphery. Low evaporation or contaminants trapped at the liquid-vapor interface might be the reason for the absence of the convective flow along the droplet free surface. A well-controlled evaporation conditions can overcome the limitations.

REFERENCES

[1] Sefiane, K.; Fukatani, Y.; Takata, Y. Thermal Patterns and Hydrothermal Waves (HTWs) in Volatile Drops. Langmuir, 2013, 29, 9750-9760.

[2] Sobac, B.; Brutin, D. Thermocapillary Instabilities in an Evaporating Drop Deposited onto a Heated Substrate. Physics of Fluids, 2012, 24, 032103(1)-(16).

[3] Zhong, X.; Duan, F. Evaporation of Sessile Droplets Affected by Graphite Nanoparticles and Binary Base Fluids. Journal of Physical Chemistry B, 2014, 118, 13636-13645.

[4] Smith, M. K.; Davis, S. H. Instabilities of Dynamic Thermocapillary Liquid Layers. Part 1. Convective Instabilities. Journal of Fluid Mechanics, 1983, 132: 119-144.

[5] Riley, R.; Neitzel, G. Instability of Thermocapillary–Buoyancy Convection in Shallow Layers. Part 1. Characterization of Steady and Oscillatory Instabilities. Journal of fluid mechanics, 1998, 359: 143-164.

[6] Garnier, N.; Chiffaudel, A. Two Dimensional Hydrothermal Waves in an Extended Cylindrical Vessel. European Physical Journal B, 2001, 19, 87-95.

[7] Riley, R. J.; Neitzel, G. P. Instability of Thermocapillary-Buoyancy Convection in Shallow Layers. Part 1. Characterization of Steady and Oscillatory Instabilities. Journal of Fluid Mechanics, 1998, 359, 143-164.

[8] Karapetsas, G,; Matar, O. K.; Valluri, P.; Sefiane, K. Convective Rolls and Hydrothermal Waves in Evaporating Sessile Drops. Langmuir, 2012, 28, 11433-11439.

[9] Carle, F.; Sobac, B.; Brutin, D. Hydrothermal Waves on Ethanol Droplets Evaporating under Terrestrial and Reduced Gravity Levels. Journal of Fluid Mechanics, 2012, 712, 614-623.
[10] Duan, F; Ward C.A. Surface Excess Properties from Energy Transport Measurements During Water Evaporation, Physical Review E, 2005, 72 (5), 056302.
[11] Duan, F; Badam, V.K.; Durst, F.; Ward CA. Thermocapillary Transport of Energy During Water Evaporation, Physical Review E, 2005, 72 (5), 056303.
[12] Duan, F; Ward C.A. Investigation of Local Evaporation Flux and Vapor-Phase Pressure at an Evaporative Droplet Interface, Langmuir, 2009, 25 (13), 7424-7431.
[13] Hu, H.; Larson, R. G. Analysis of the Effects of Marangoni Stresses on the Microflow in an Evaporating Sessile Droplet. Langmuir 2005, 21, 3972-3980.
[14] Garnier, N. Ondes non-lineaires a une et deux dimensions dans une mince couche de fluide. Ph.D. dissertation, 2000.